Jour.Korean Inst. Mining Geol.
Vol. .24, No.4, p.421-434,1991.

Magnetic Investigation of the Yangsan Fault

Byung - Doo Kwon* and Ki - Won Lee*

ABSTRACT : Ground magnetic surveys were conducted at four areas where the Yangsan fault , the most prominent lineament in the Kyeongsang basin, appears to be passed through. For data processing, IGRF correction, upward continuation and reduction-to-the-pole were performed. The automatic inversion by using a matrix computation method, which takes the depth to bottom layer of the horizontal two layer structure as the model parameter, has been attempted to delineate the subsurface structure. Upward continuation of the surface magnetic map to the same level of the aeromagnetic survey (KIER,1989) resulted in very similiar patterns to those of aeromagnetic data. Subsurface modeling of eight profile data show that the strike and dip of the Yangsan fault in study areas are N 6° −15° E, and near vertical to somewhat eastward, repectively , despite of the local lithological contrast of each study area. It seems that the magnetic effect of faulting in the study area 1, which locates in the most northern part of the survey areas, is disturbed by that of igneous intrusion. At study area 2, the possibility of volcanic or igneous intrusion, which is 200-300 meters wide along the fault plane was presented. At study area 3, unlike other study areas, distinct fracture zone of 500-700 meters in width was revealed along the surface fault line. The andesitic rocks of the study area 4 have very high susceptibilities and the fault line on surface of this area was shifted about 500 meter eastward, as compared with the inferred fault line by the previous study.

INTRODUCTION

The Yangsan fault is located in the eastern part of the Kyeongsang basin and is clearly seen on the large scale geologic maps (such as 1 : 250,000 scale) and on the lineament maps which are based on the Landsat image data (Kang, 1979). Nearby this fault, there are the series of faults such as the Dongrae and the Ilkwang faults whose strikes are nearly parallel to that of the Yangsan fault. The Yangsan fault appears to be extended from northern part of Angang-eub in the Kyeongsangbuk-do to the southern part in the vicinity of Yangsan-gun in the Kyeongsangnam-do. Several geological and geophysical studies have been conducted on the Yangsan fault to elucidate the structure and movement of the fault(Park, 1984 ; Kim, 1984 ; Lee et al., 1984 ; Kim, 1985 ; Lee et al., 1985, 1987 ; Min et al.,1985, 1987, Kim et al.,1990). They have reported that the Yangsan fault has developed relatively wide fracture zone along the fault line, which is associated with the thick sedimentary layer or Quartenary alluvium. Also, the patterns of severe variations are observed on geophysical anomalies and physical properties of rocks in the vincinity of the fault zone. However, there are still controversial opinions about the extent and type of the fault. In this study, we have carried out the ground magnetic surveys at four areas(Fig.1), where the Yangsan fault appears to pass through, to investigate magnetic characteristics and probable subsurface structure of the fault. The location, strike, and dip of the Yangsan fault are deduced by analyzing the magnetic anomaly maps and the subsurface structures obtained by inversion process.

* Department of Earth Sciences, College of Education, Seoul National University, Seoul, 151-742 Korea.

OVERVIEW OF THE GEOLOGY

The geology of the Yangsan fault zone is closely related to the development of the Kyeongsang basin which contains a massive sequence of the non-marine sedimentary rocks and a large volume of igneous rocks.

Before the fault development or at the same time of the faulting, the lithological features around the Yangsan fault, such as sedimentary formations, pre-Cretaceous basement rocks and its structural geology, had been changed by several episodes of volcanic and plutonic activities from middle Cretaceous to late Cretaceous or early Tertiary. Based on studies of Lee and Ueda (1976), Otsuki and Ehiro (1978) report that the Yangsan fault is the right-lateral strike slip fault, with a displacement of approximately 25 km, and faulting activity had continued from Paleocene (60 My BP) to Oligogocene (30 My BP), reaching its climax in Eocene of Tertiary. Min et al.(1982) has suggested that the Yangsan fault began to develop after late Cretaceous. Meanwhile, as the

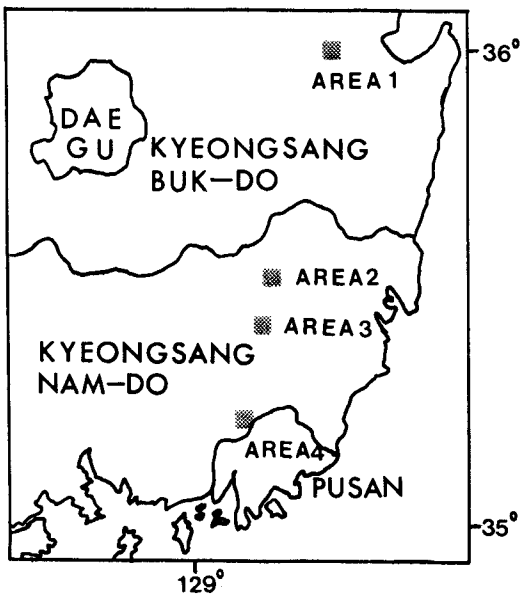

Fig. 1. Location of magnetic survey areas.

Area 1 ; Dangu-ri and Dasan-ri, Gangdong-myon, Woelsung-gun, Kyeongsangbuk-do,
Area 2 ; Jikdong-ri, Eonyang-myon, Woolju-gun, Kyeongsangnam-do,
Area 3 ; Yongyeon-ri, Sangbuk-myon, Yangsan-gun, Kyeongsangnam-do,
Area 4 ; Bomo-ri, Mulgum-myon, Yangsan-gun, Kyeongsangnam-do.

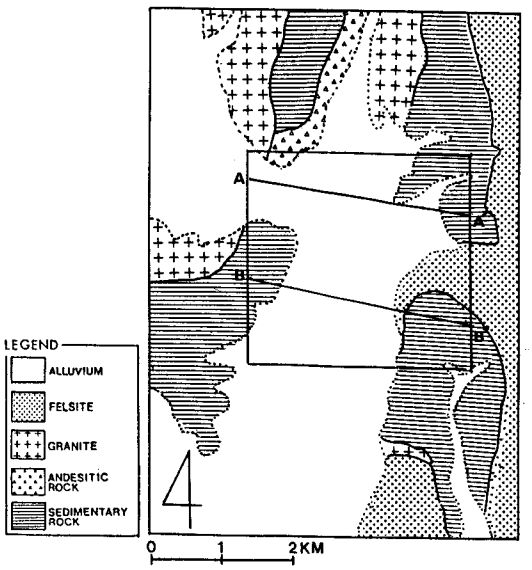

Fig. 2. The simplified geologic map of the study area 1 (after Kim et al., 1971). Rectangle represents the surveyed area. Profiles AA' and BB' are selected for subsurface modeling.

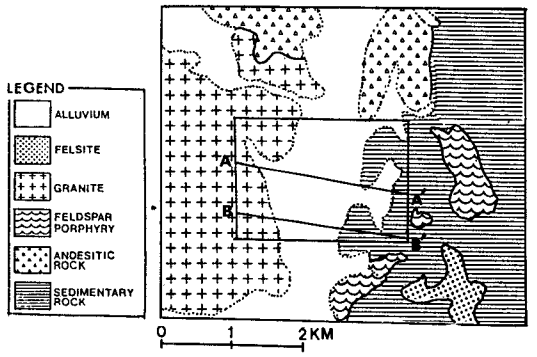

Fig. 3. The simplified geologic map of the study area 2 (after Lee and Lee, 1972).

results of the tectonic lineament studies, Lee(1974) correlated the Yangsan fault with a dip fault trending east of Taiwan through Cheju island to Ulreung island. Choi et al.(1981) has proposed the possilibity that the Yangsan fault is one sort of the hinze fault whose eastern block has been risen in the southern part of the fault and has been fallen in the northern part of Kyeongju.

Simplified geologic maps of four survey areas are illustrated in Figs. 2 - 5. It can be seen that major rock types of the Yangsan fault zone are granite and andesitic rocks in the western parts and sedimentary rocks in the eastern parts along the fault line. The sediments exhibit a kind of the molasse type consisting of the conglomerate, sandstone, shale and some pyroclastics, and have been differentiated into various sedimentary formations during the Cretaceous. Therefore, near-surface and surface part of the basin is mostly composed of the volcanic and igneous rocks and volcanoclastic materials with clastic sediments. However, the geological boundary between igneous and sedimentary rocks is obscured due to thick Quaternary sediments and the strong disturbances caused by igneous intrusion.

MAGNETIC MEASUREMENT

Through the regional reconnaissance survey of the Yangsan fault area,four appropriate study areas, which represent northern, middle and southern part of the fault, were selected for

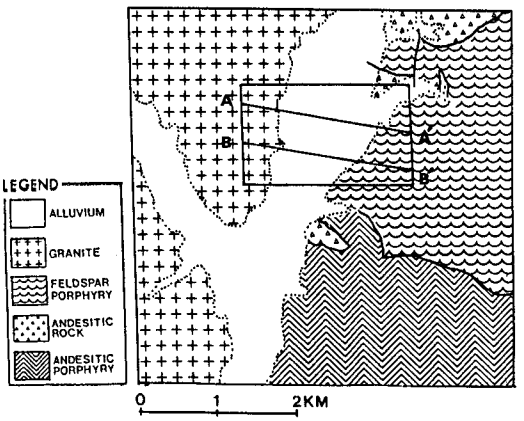

Fig. 4. The simplified geologic map of the study area 3 (after Lee and Lee, 1972).

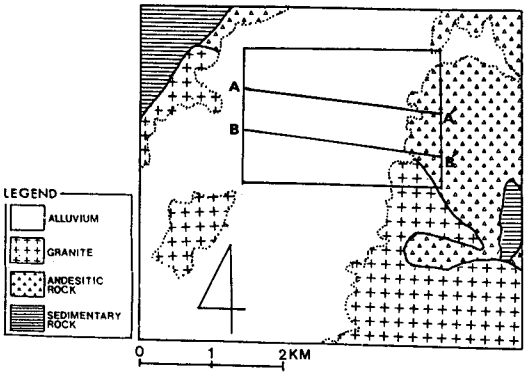

Fig. 5. The simplified geologic map of the study area 4 (after Lee and Kang,1964).

magnetic surveys. The MP-2 proton magnetometers of Scintrex Co. were used to measure strengh of the total magnetic field, and a G-866 proton magnetometer of Geometric Inc. was also set up to measure daily variation of the geomagnetic field. Measurements were made at 919 observation points in the study area 1, 234 points in the area 2, 176 points in the area 3, and 300 points in the area 4. Magnetic suscepibilities of the rock specimens were measured by MS-3 Bridge of Geometric Inc. and CPU-2 of Scintrex Co. The Kappameter was also used in the field to assure those values. At the study area 1, suscepibilities of granite samples are in the range of 0.0004 - 0.0015 cgsemu (Fig. 6(a)) and those of sedimentary rock shows its maximum value of 0.0005 cgsemu. In case of the area 2, maximum suscepibility of granite sample is 0.

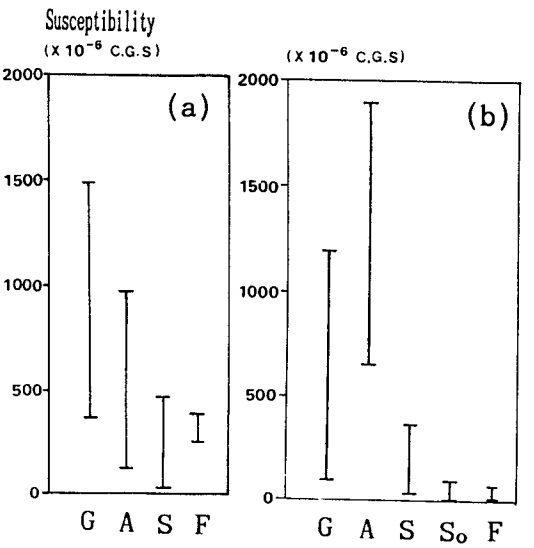

Fig. 6. Susceptibility range of rock samples in study area 1 (a) and 2 (b). G ; Granite, A ; Andesitic rock, S ; Sedimentary rocks, F ; Felsite, So ; Soil.

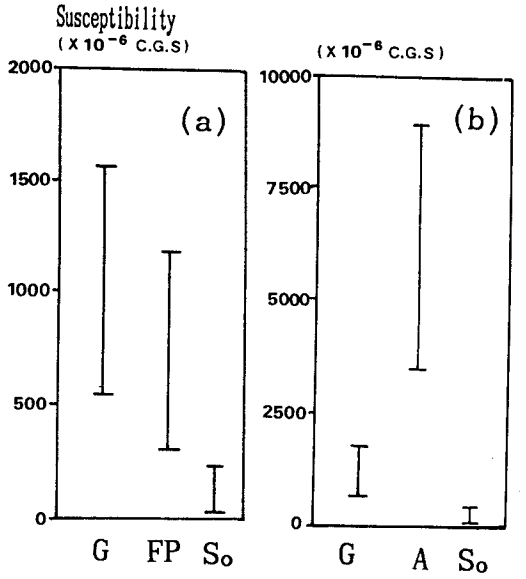

Fig. 7. Susceptibility range of rock samples in study area 3 (a) and 4 (b). G ; Granite, A ; Andesitic rock, FP ; Felspar porphyry, So ; Soil.

0012 cgsemu and susceptibilities of andesite samples are in the range of 0.00065-0.0018 cgsemu(Fig. 6(b)). And Susceptibilities of granite samples and feldspar porphyries in the study area 3 are 0.0006-0.0016 and 0.0003-0. 0016 cgsemu, respectively(Fig. 7(a)). In the

study area 4, andesite samples show very high suscepibilities of 0.003-0.008 cgsemu(Fig. 7(b)).

DATA PROCESSING AND INTERPRETATION

IGRF Computation For Normal Correction

IGRF (International Geomagnetic Reference Field) computation at each station is necessary for so-called normal correction (Nettleton, 1976), which removes spatial variation of the magnetic field due to the earth's inner source from the observed data. This corresponds in a general way to the latitude correction of gravity data. The mathematical expression for normal correction is based on the theoretical aspects that the strength of the geomagnetic field and its inclination and declination at any point can be computed by using the Gauss coefficients (Barraclough, 1985) obtained from spherical harmonic analysis of the magnetic data of the global size. For computation of IGRF, the algorithm proposed by Mailn and Barraclough (1981) is used. Since the survey areas are relatively small, we have computed the IGRF only at the central point of the each surveyed area (Table 1).

Total field intensities and inclinations of the geomagnetic field at four positions show a nearly linear trend of northward increasement, and declinations at four positions are about 7 degrees west of north.

Table 1. The result of the IGRF computation at the center of each survey area

Study Area	Area 1	Area 2	Area 3	Area 4
Co-latitude(°)	53.70	54.42	54.83	55.02
Longitude(°)	129.15	129.13	129.04	129.03
Total Field(γ)	49469.56	49059.83	48846.90	48746.39
Inclination(°)	51.61	50.68	50.16	49.92
Declination(°)	-7.29	-7.05	-6.91	-6.85

Upward Continuation

Upward continuation of the ground magnetic data is sometimes used to suppress the component of magnetic noise caused by unwanted sources of near surface such as low-pass filtering. For continuation processing of potential data, Henderson's method (Lagrangian interpolation) and spectral method (frequency domain analysis) have been generally used (Kwon ,1981). We have adopted the former method to avoid the oscillation effect which may be caused by discontinuities of anomaly values at the edges of the study area. The upward continuation processing in this study has dual purposes as follows; firstly, for qualitative trend analysis of the fault line on the 2-dimensional anomaly map and secondly, for comparison with aeromagnetic data (KIER, 1989) to evaluate the

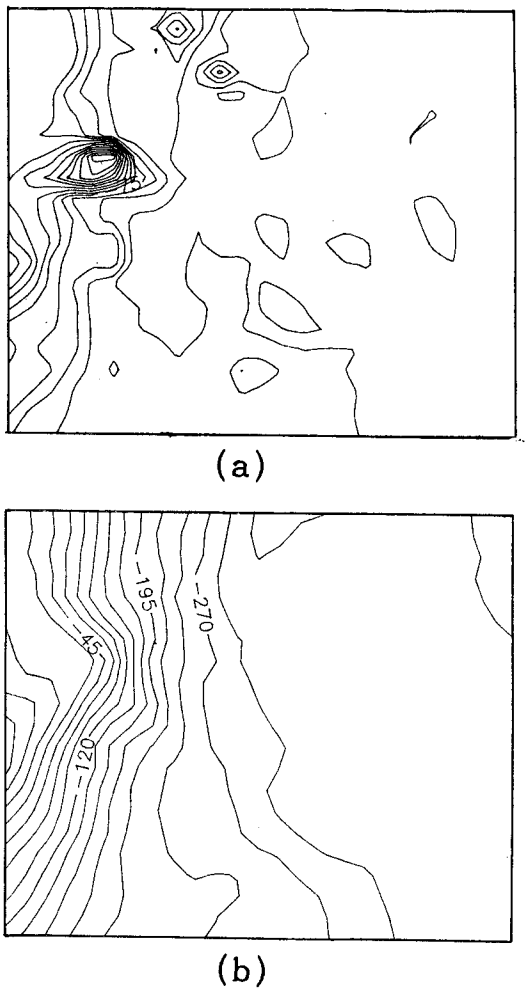

Fig. 8. Surface magnetic anomaly map (a) and its upward continued map (b) in the study area 1. Contour intervals are 50 gammas for (a) and 25 gammas for (b).

quality of ground magnetic survey data. At the study area 1, the upward continued map shows a visible linear trend of N-S direction with high anomaly values in the western part (Fig. 8 (b)). This pattern is a nearly typical one expected from a fault-bearing structure.

Fig. 9 compares the upward continued map of the study area 2 with the aeromagnetic map published by Korea Institute of Energy and Resources(1989). The linear fault trend of N 10° -20° E in the south-eastern part of the map is relatively clear and the fault line in this area appears to be the boundary between granitic block in western part and sedimentary rocks in eastern part. However, the inference of fault location and its strike is slightly complicated by nearby anomalies of circular pattern which might be related to a dike or a volcanic intrusion. The aeromagnetic map shows a rather simple pattern, from which the strike of the fault may be identified as nearly N-S trend(Fig. 9(c)). In the study area 3, western granitic body and eastern porphyritic body show nearly similiar ranges of susceptibility. Therefore, the fault location is inferred along the linear trend showing the sharpest gradient of anomaly values at the central part(Fig. 10(b)). From the upward continued map, the dominant strike of the fault appears to be approximately N15° E. However, the distinct trend related to the fault structure is not well identified from aeromagnetic map, because it might be highly disturbed by uncertain sources in south-eastern portion(Fig. 10(c)).

Both the upward continued map and the aeromagnetic map of the study area 4 show

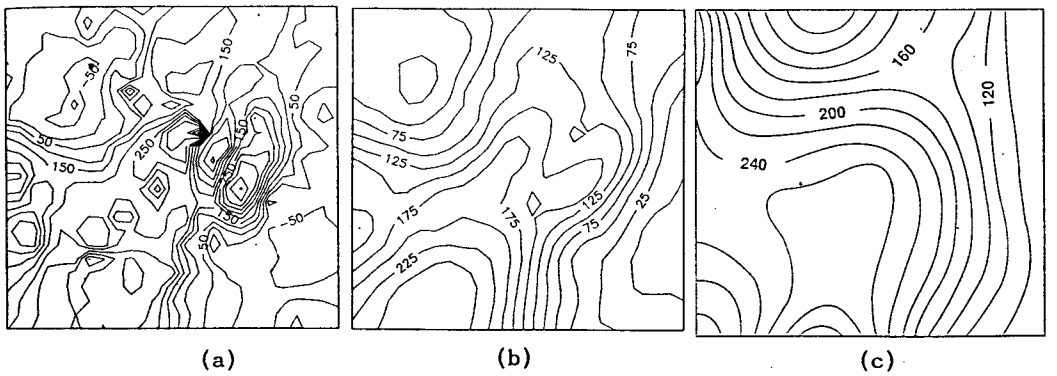

Fig. 9. The surface magnetic anomaly map (a), the upward continued map (b) in the study area 2 and the actual aeromagnetic map (c) from KIER(1989) in the same region. Contour intervals are 50 gammas for (a) and 25 gammas for (b) and 20 gammas for (c).

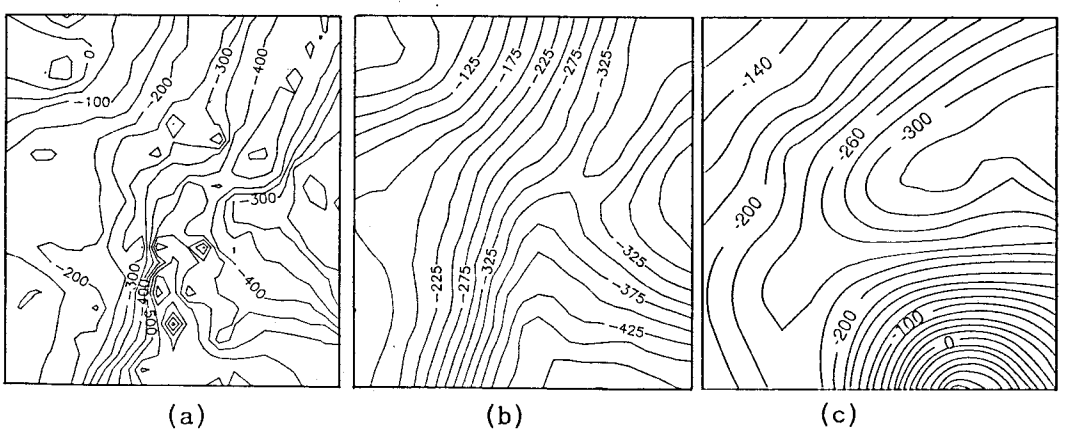

Fig. 10. The surface magnetic anomaly map (a), the upward continued map (b) in the study area 3 and the actual aeromagnetic map (c) from KIER(1989) in the same region. Contour intervals are 50 gammas for (a) and 25 gammas for (b) and 20 gammas for (c).

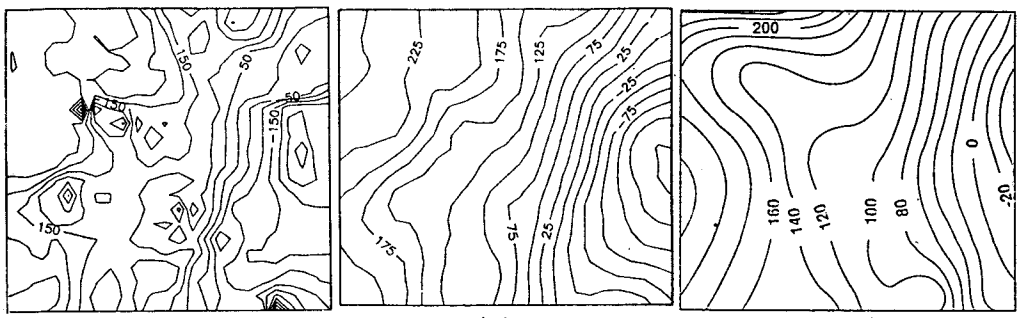

Fig. 11. The surface magnetic anomaly map (a), the upward continued map (b) in the study area 4 and the actual aeromagnetic map (c) from KIER(1989) in the same region. Contour intervals are 50 gammas for (a) and 25 gammas for (b) and 20 gammas for (c).

similiar trend, but slightly different range of anomaly values(Fig. 11). However, the strike of the fault in this area is relatively apparent in the eastern part of the upward continued map as N15° -20° E. In general, upward continued maps and aeromagnetic maps show similiar patterns in most surveyed area, but some differences in field values and local patterns. These differences seems to be affected mainly by the factors such that the upward level at each study area is not perfectly same and that rather different methods are used for data processing and contouring technique.

Reduction to the Pole

The shape of total magnetic anomalies are affected by the directions of magnetization of source bodies and the earth magnetic field vectors. Except when inclination is either 90° or 0°, the magnetic anomalies show rather complicate shapes, thus it is difficult to interpret every single anomaly in related with the causative geologic bodies. Therefore, RTP (Reduction to the pole) processing has been commonly used to remove the dependence of the magnetic data on the angle of magnetic inclination at the magnetic anomaly map.

Because we have dealt with profile data traversing inferred fault, we have modified expressions of classical RTP method developed by Bhattacharyya(1965) as followings.

The Fourier transform F(k) of magnetic field f (x), for 1-dimensional case, may be expressed as,

$$F(k) = \sum_{x=0}^{N-1} f(x) \exp(2\pi ikx / N) \qquad (1)$$

for $k = 0, 1, 2, 3, \ldots\ldots, N-1$

$x = 0, 1, 2, 3, \ldots\ldots, N-1$

The magnetic field reduced to the pole ,Tr, is obtained as follows,

$$T_r = \frac{1}{\sin I \sin I_o} \sum F(k) \exp(Pz)\, R(k) \exp(Pixk) \qquad (2)$$

where

$$P = 2\pi / NK$$

$$R(K) = \frac{P^4 \varphi_1 \varphi_2 P^2 - i(\varphi_1 + \varphi_2) P^3}{(P^2 - \varphi_1 \varphi_2)^2 - (\varphi_1 + \varphi_2)^2 P^2}$$

$$\varphi_1 = P / \cot I_{or} \cos D_o$$

$$\varphi_2 = P / \cot I_o \cos D$$

$$I_{or} = 180° - I_o$$

$$I_o = 180° - I$$

$$I_o = I \text{ and } D_o = D$$

I and D are the inclination and declination of magnetization, and I_o and D_o are those of the earth's normal field. To simplify the problem, we assume that

$$I_o = I \text{ and } D_o = D$$

and I and D are thought to be available as the result of IGRF computation of each survey area(Table 1). The eight profiles selected from the anomaly maps and their RTP results are shown in Fig. 12. In general, the RTP profiles show

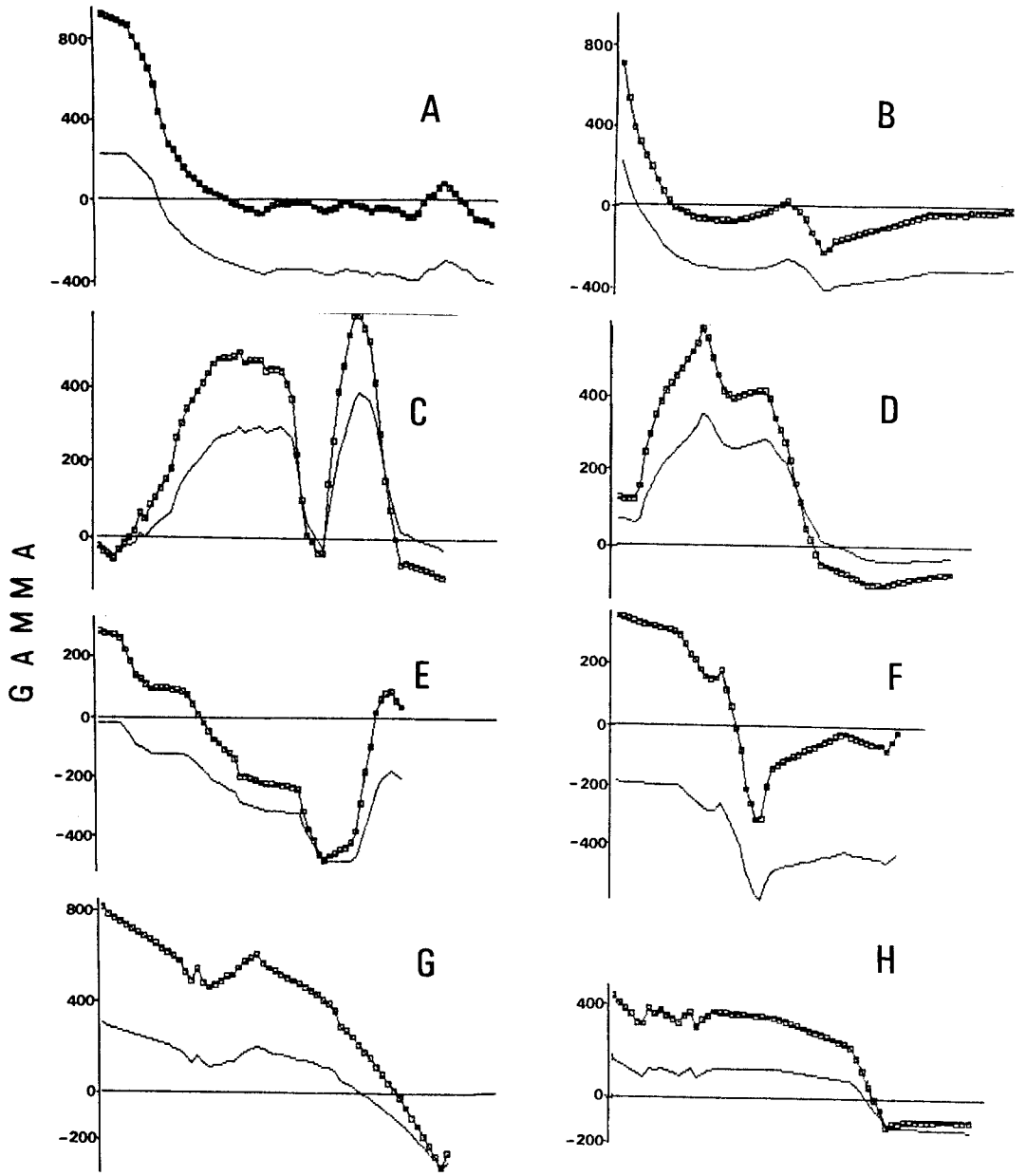

Fig. 12. The observed profiles (solid line) and their corresponding RTP profiles (line with rectangles). A and B ; AA' and BB' profiles of the study area 1,C and D ; AA' and BB' profiles of the study area 2, E and F ; AA' and BB' profiles of the study area 3, G and H ; AA' and BB' profiles of the study area 4.

similiar trends to those of original observed data, but the marked increase of variation of anomaly values is shown in them. These profiles are used for subsurface modeling of the fault.

Iterative Depth Inversion for Subsurface Modeling

For quantitative interpretation of subsurface

structure originated from faulting, the iterative matrix inversion of the depth parameter using 2-dimensional rectangular block model(Bott,1973 ; Lee et al., 1985) is used in this study. As for this method, the prism models to be used for depth inversion are shown in Fig.13. The magnetic effect(Δ m) due to a horizontal rectangular prism(Fig.13 (a)), is given as follows :

$$\Delta m = 2FM \{\log\left(\frac{R_B R_D}{R_A R_C}\right) \sin\beta + (\phi_{CD} - \phi_{BA}) \cos\beta\} \quad (3)$$

where

$$F = (\sin^2 I_m + \cos^2 \alpha_m)(\sin^2 I_o + \cos^2 I_o \cos^2 \alpha_o)$$

$$\beta = \tan^{-1}(\tan I_m / \tan \alpha_m) + \tan^{-1}(\tan I_c / \tan \alpha_e)$$

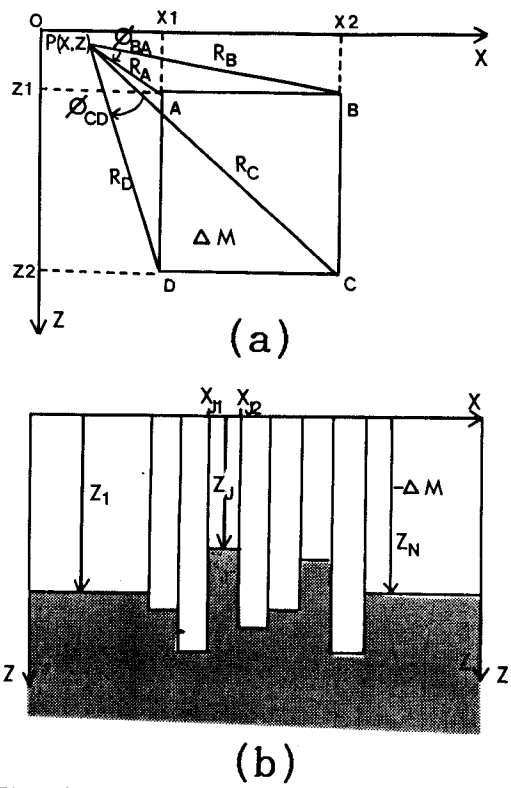

Fig. 13. Prism model for depth inversion of magnetic data.(a) : Single 2-dimensional prism for computing total magnetic field, (b) : 2-dimensional depth model.

and M is the magnetization and I_m and I_e are the dip of the direction magnetization and of the measured anomaly component, respectively, and α_m and α_e are the corresponding azimuthal directions determined from the positive x-axis. The j^{th} elements of Jacobian matrix (J) for non-linear inversion are given by taking partial derivative of eq.(3) with respect to depth parameter (∂ z),

$$\frac{\partial m}{\partial z} = 2F\Delta M \{Z(\frac{1}{R_{jD}^2} - \frac{1}{R_{jC}^2}) \sin\beta + (\frac{1}{R_{jB}^2} - \frac{1}{R_{jA}^2}) \cos\beta\}$$

$$\mathbf{J} = \left.\frac{\partial m}{\partial z_j}\right| \quad j = 1, N$$

Therefore, the depth parameter can be computed as J^{-1} ε , where ε is the difference between measured and calculated field values. Meanwhile, J is expressed in matrix notation as follows :

$$\mathbf{J} = \mathbf{USV}^T$$
$$\partial z = \mathbf{VTS}^{-1}\mathbf{U}^T\varepsilon \quad (5)$$
$$\mathbf{T} = (\mathbf{S}^2 + \nu^2\mathbf{I})\mathbf{S}^2$$

where **U** and **V** are orthogonal matrices and **S** is the diagonal matrix of the singular value of **J**, and **T** is a diagonal matrix of N x N , which is associated with the damping factors and ν^2 is a second order of Marquardt variables. In case of the 2nd order Marquadt variable, the element of T is given by

$$t_i^L = \frac{k_i^{2L}}{k_i^{2L} + \mu^{2L}} \quad \text{for } i = 1, P$$

where $k_i = s_i / s_i, \mu = \nu / s_1$, s_1 is the maximun singular value.

Finally, the depth parameter can be calculated as follows :

$$\partial z = \mathbf{VT}^L \mathbf{S}^{-1} \mathbf{U}^T \quad (6)$$

Study Area 1

In the study area 1, maybe situated in the northern portion of the Yangsan fault, the location of the fault does not clearly appear in the geologic map (Fig.2). Several geophysical

studies were carried out in the nearby this area. Min and Chung(1985) estimated that the depth to bedrocks around this area was about 3.8 km by analyzing their gravity study. Lee et al.(1986) carried out eletrical resistivity surveys and reported the appearence of low resitivity zone, as a sector of the Yangsan fault line extended to the southern part of the fault. Also, Lee et al. (1990) presented the possibility that the fault line would be shifted approximately 500 meters eastward compared with the inferred fault line traversing the central portion in the geologic map (Fig. 2), though the faulting trend of this area was extended along the strike of N20° E.

From upward continued map(Fig. 8(b)), the location and strike of the fault are qualitatively revealed by the appearence of linear trends which might depend partly or mostly on the faulting structure, though the informations about the fault nature such as dipping plane, movement, and type are not directly derived from the map. For quantitative interpretation

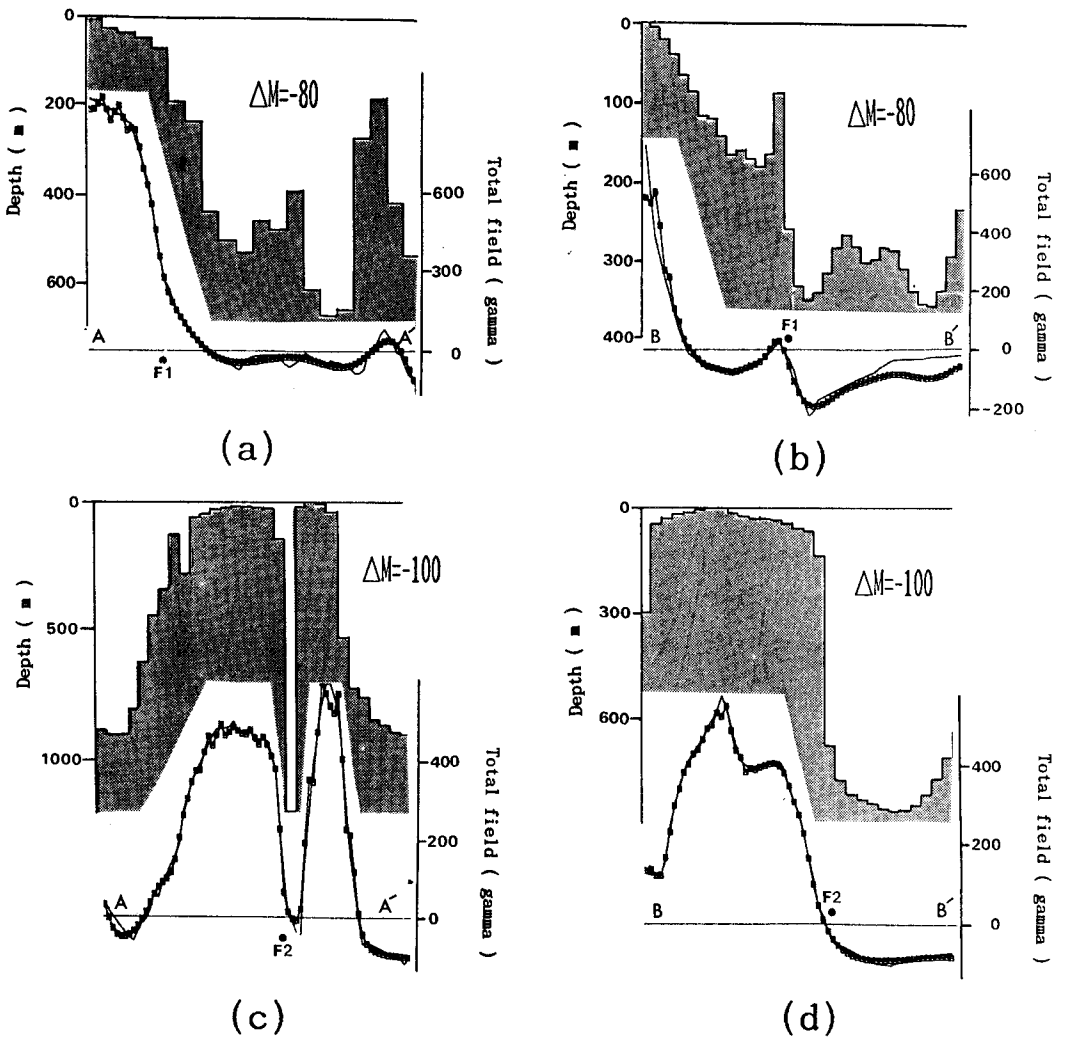

Fig. 14. The results of depth inversion for subsurface modelling. (a) and (b) are the profiles AA' and BB' of the study area 1, (c) and (d) are the profiles AA' and BB' of the study area 2. The solid lines indicate the RTP profiles of the observed field and the solid lines with rectangules indicate the profiles of the computed field from the model. △ M are the total magnetic field in gamma unit, and F1 and F2 indicate fault locations determined in this study.

about the subsurface structure related to the faulting in this area, two profiles (AA' and BB' of Fig. 2) across the apparent linear trend of magnetic anomalies (Fig.8(b)) are chosen. Since the automatic inversion method adopted in this study takes a model parameter as the depth to the top of the magnetized bodies,, it requires initial guess as magnetization contrast between two layers. For this simplified structural setting, it is assumed that lower layer is composed of the bedrocks or igneous rocks of high susceptibilities, and upper layer contains low magnetic materials such as unconsolidated alluvium, sedimentary rocks and felsite, in case of this area. The magnetization contrast between two layer is calculated as approximately 80 gammas by multiplying the susceptibility values and total magnetic field strength of this area(Table 1 and Fig. 6(a)). But it is thought that the magnetic effects due to the the fault are likely to be distorted in the western part along the fault line, where massive granitic intrusion are

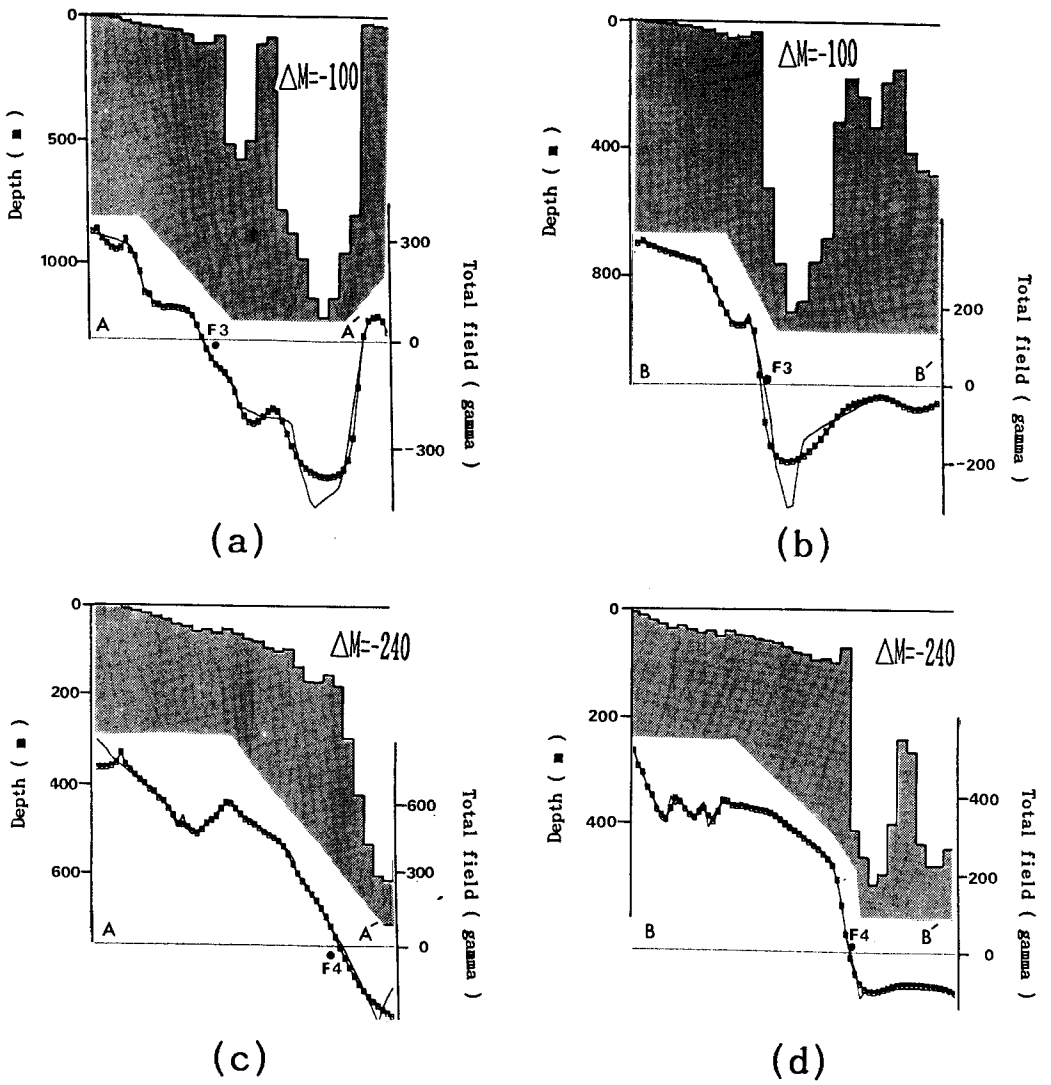

Fig. 15. The results of depth inversion for subsurface modelling. (a) and (b) are the profiles AA' and BB' of the study area 3, (c) and (d) are the profiles AA' and BB' of the study area 4. Symbols are as same as those used in Fig.14.

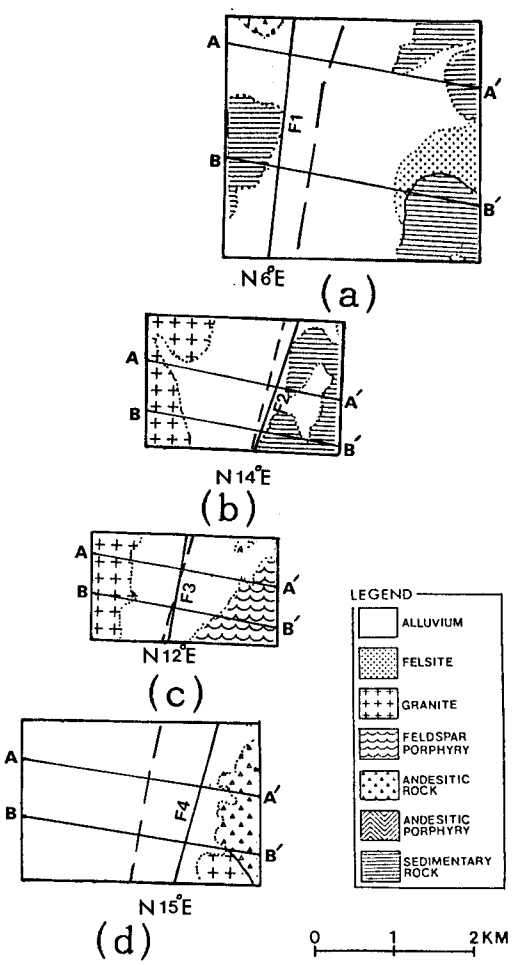

Fig. 16. Illustration of the fault lines at surface in the study areas. Solid lines indicate the fault line determined based on the results of Figs. 14 and 15 in this study. Dashed lines represent the fault line of the previous studies.

occured(Fig. 2). This preconceived idea is well verified from the result of inversion at Fig. 14 (a) and (b). In addition to this obscure aspect against interpretation of the fault nature, the very small contrast of susceptibilities between felsite and sedimentary rocks also makes it difficult to quantitatively interprete the feature of the fault and its surrounding geologic characteristics around this studied area.

However, the dip of the fault in this area seems to be 70° -90° to the east, judging from probable fault positions (F1 points) selected on AA' and BB' profiles (Fig. 16(a)). The strike of the fault is identified as N 6° E.

Study Area 2

In this area, several geophysical surveys have been previously performed by Kim (1982), Lee et al.(1984) and Kim (1985). Kim (1982), through his magnetic study , reported that magnetic anomaly patterns were partly governed by the intrusion of magnetized body of rather high susceptibility, which are not exposed on the geologic map(Fig. 3). Lee et al.(1984) proposed that a kind of wide fracture zone had developed along the fault line, but sharp gradient of gravity anomaly ,which might generally be associated with the fault structure, was not shown in their study. And, Kim(1985) suggested that the dip of the fault was slightly vertical, by analyzing his electric resistivity survey data. Nevertheless, all these previous studies are in accord with the the direction of the strike of the fault as N 15° - 25° E.

For inversion procedure, the rock types of the upper and the lower layer are thought as same as those of the study area 1, because the geologic setting in both areas is similiar. However, the range of bulk rock susceptibilities within two areas is rather different (Fig. 6), especially in case of andesite. The susceptibility band of andesite samples from this area is much higher than that of study area 1. It is thought that this fact is attributed to mainly differential erosion and partly rock type itself, because some difference in mineral composition of andesites are observed in both rock samples and outcrops between these areas which are apart more than 15 km. Therefore, the highly magnetized lower layer is adopted to be composed of granites , andesitic rocks and other bedrocks, and the magnetizaton contrast is taken to be 100 gamma assuming that the magnetization of the upper layer is nil. Fig. 14(c) and (d) show the results of the depth inversion for profiles AA' and BB'. The points, F2, indicate the fault locations. The fault location on the profiles BB' is rather evident, but some ambiguities arise in determining the fault location on the profile AA'.

To explain these ambigous aspect in profile AA', two probable hypotheses can be considered. One is based on concentration of magnetic minerals along weak fracture zone associated with faulting movement on this area (Olorunfemi et al., 1986) and the other is a simple dike model(Kim, 1982). The former idea seems to be less reasonable because its characteristic feature is not shown in the profile BB'. Therefore, it is said that the intrusion of

small dike, which is revealed as the width of approximately 300 meters, along the fault is more valid, judging from only this magnetic study.

The fault line determined in this area (Fig. 16) is consistent with that provided in previous studies. The strike of the fault seems to be N 14° E and the fault plane appears to be nearly vertical in this area.

Study Area 3

Kim(1984) conducted the eletric resistivity survey, which is the only geophysical study previously carried out in this area, and reported the dip of the fault was rather westerly or nearly vertical. He also reported the existence of low resistivity zone along the fault line. It can be said that this region is not so favorable for ground magnetic study because susceptibility contrast between rock types is not so apparent (Fig. 7 (a)) and diamagnetic feature of water-bearing ravine, though shallow, is observed in the central portion of this area. The upward continued magnetic anomaly map (Fig. 10), however, reveals the linear pattern which may be due to the faulting movement and the low magnetic zone in central part of this study area, which is well appeared in the profile data of Fig. 15 (a) and (b) and may correspond to the low resistivity zone of Kim(1984).

The extent of this low magnetic zone is deduced by depth inversion assuming 100 gammas as magnetization contrast between the upper and the lower layer. In the profiles AA'and BB', the sizes of this zone are approximately 800 m and 500 m wide, respectively. These zones are thought as a local fracture zone of the Yangsan fault, judging from their trends and surrounding geologic features, though the reason why the fracture zone has low magnetic characteristics is not readily explainable at this study. It is shown that the strike of the fault is N12° E , which is nearly same as that of the northern part of the Yangsan fault (Fig.16 (c)). The average width of fault fracture zone in this area appears to be nearly 650 m, and the lithological boundary between granitic block and porphyritic rocks in the fracture zone cannot be clearly defined because susceptibilities of both rocks show similiar range of values(Fig. 7(a)). Based on the fault point (F3) on Fig. 15 (a) and (b), the dip of the fault appears to be nearly vertical.

Study Area 4

Min and Kim (1987) suggested that the depth to the basement is 3.3 - 5.2 Km around this area, through the spectral analysis of their gravity data obtained on a large profile. The geology around this area is quite complicated because of wide and thick Quarternary alluvium, various sedimentary formations and andesitic rocks.

The andesitic rocks show much higher susceptibility in comparison with that of andesitic rocks in other study areas(Fig.7(b)) and are probably affected by IRM (Isothermal Remanant Magnetization)(Chapman and Bartels, 1940). Taking into account these complexity on geologic aspects , the determination of magnetic basement is not so simple, either. Nevertheless, the upward continued map (Fig.11) and the RTP profiles (Fig. 12) show the typical characteristic patterns associated with faulting. The magnetization contrast for depth inversion is taken as 240 gammas because ubiquitous andesitic outcrops cannot be totally ignored during the modeling procedure. From the point, F4 , on the profiles AA' and BB' (Fig. 15 (c) and (d)), the strike of the fault in this region is delineated as N 15° E, which is analogous to that of the study areas 2 and 3. The dip of the fault within the subsurface can be presented as easterly 80°-90°, which is analogous to that of the study area 1. However, the location of the fault in this area on the surface appears to be shifted 500 meter eastward as compared with that proposed in the previous study.

CONCLUSIONS

The ground magnetic surveys are conducted at four areas along the Yangsan fault. To examine the validity of ground data, a direct comparison with the aeromagnetic surveyed data was made by upward continuation process. Two data sets coincide with each other in their anomaly shape quite well, though local differences are sometimes observed.

Therefore, if irrelevant noises observed in the ground survey could be properly eliminated, the ground survey data would be prefer to the aeromagnetic data, in case that a more detailed geologic interpretation is required.

The susceptibilities of granite samples in the study area 1 are 0.0004-0.0015 cgs emu and that of sedimentary rocks shows the maximum value of 0.0005 cgs emu. In case of the study area 2, maximum susceptibility of granite samples is 0. 0012 cgs emu and the susceptibility of andesite is 0.00065 -0.0018 cgs emu. And in case of the study area 3, susceptibility of granite is 0.0006 - 0.0016 cgs emu and susceptibility of feldspar porphyry is 0.0003-0.0016 cgs emu. The

suscepibility of andesite in the study area 4 appears to be very high, as 0.003- 0.008 cgs emu. For subsurface modeling of the fault structure, the automatic non-linear matrix inversion method by adopting the model parameter of depth with a Marquardt damping factor is used. The thickness of the upper layer, which is assumed to be composed of Quaternary sediments or of sedimetary rocks which have formed since Pre-Cambrian period and of clasts generated from strong faulting movement, appears to be 50 - 650 m in the study area 1, northern portion of the Yangsan fault. In the middle part of the fault, such as the areas 2 and 3, it is from nil to 800 - 1000 m, at maximum, and in the southern part as the study area 4, it is from nil to 500- 600 m. These results seems to be in accord with results of the probable sedimentations associated with the tectonics of the southeastern of Korea(Chang, 1978). The dip of the fault appears to be nearly vertical in the study areas 2 and 3 and seems to be rather easterly in the study areas 1 and 4. The lineament of N 6° -15° E represents as a dominant trend in the whole study areas.

As for the characteristics of magnetic anomalies, linear trends are well appeared on all the study areas, which may indicate the existence of the fault. Especially the low magnetization zone in the study 3, might be related to the fracture zone which may be closely associated with the development of the faulting. The isolated high anomaly in the study area 2 seems to be associated with the igneous or plutonic intrusion whose relationship with the faulting is rather ambiguous. In the case of the study areas 1 and 4, simple typical patterns originated from faulting movement are shown, but any visible isolated features are not appeared. High magnetic anomalies are occasionally observed in the fracture zone(Olorunfemi et al., 1986), where the mineral concentration is occurred along the fault plane, but these kind of high anomaly zone is not seen at the Yangsan fault.

In general, the magnetic survey alone in relatively small area, where only strike-slip movement is involved, provides very limited information about fault characteristics, the fracture zone. Moreover, if the faults movement of the strike slip is concomitant with the vertical movement by faulting mechanism or tectonic uplifting, the interpretation about the fault nature is likely to be more difficult and to be more ambiguous.

However, formation of subsurface structures, which are obtained by inversion of observed anomalies at four areas in this study, seems to be rather well explained if the Yangsan fault had been accompanied by the vertical motion , more or less, along with a well-known large strike-slip motion. In this fault, the vertical motion might be caused by structural uplift associated with the igneous activities.

The Yangsan fault reveals typical feature in the strike of NE on all magnetic anomaly maps quite clearly, and the dip of the fault appears to vary from slightly eastward to vertical, not to westward.

ACKNOWLEDGEMENT

This article is presented as a part of " A geomagnetic study of theYangsan fault area " which is supported by the Korea Science and Engineering Foundation.

REFERENCES

Barraclough, D.R.(1985) Scientific Note : International Geomagnetic Reference Field Revision 1985. Pure and Appl. Geophy.,v.123, p. 641-645.

Bhattacharyya, B.K.(1965) Two-dimensional harmonic analysis as a tool for magnetic interpretation.Geophysics,v.30,p.829-857.

Bott, M.H.P. (1973) Inverse methods in the interpretation of magnetic and gravity anomalies, in Methods in Computational Physics , Bolt,B.A.(ed.), p.133-162.

Chapman, S and Bartels, J.(1940) Geomagnetism. Oxford Press, p.144-146.

Chang, K.H.(1978) Late Mesozoic Stratigraphy, Sedimentation and Tectonic of Southeastern Korea (II) - with discussion on petroleum possibility.Jour. Geol.Soc.Korea,v.14,p.120-135(in Korean).

Choi, H.I., Son, J.D. and Oh, J.H. (1981), Sedimentology and stratigraphy of the Cretaceous Gyeongsang strata, United Nations ESCAP, CCCP Technical Bulletin,v.14.

Kang, P.J.(1979) Geological Analysis of Landsat Imagery of the South Korea.Jour. Geol.Soc. Korea, v.15,p.181-191(in Korean).

Kim,N.J., Kwon,Y.L. and Jin, M.S.(1971) Explanatory text of the geological map of Moryang sheet(1: 50000). Geological Survey of Korea.

Kim, Y.H.(1982) A geophysical study of the geologic structure on Eonyang area, south-eastern Korea. M. Sc.thesis , Seoul National University,32p.

Kim, Y.H.(1985) The geoeletric study on the Yangsan fault, Ph.D. dissertation, Seoul National University. 72p.

Kim, Y.H, Lee, K.H. and Seong I.K. (1990) A Geoelectric Study on the Yangsan Fault, North of Kyeongju. Jour.Geol.Soc.Korea, v.26, p.393-403(in Korean).

Korea Institute of Energe Resources (1989) Studies

for the Exploration of Mineral Deposits. KR-88-2D-1,p.21-22(in Korean).

Kwon, B.D.(1981) Comparative studies of methods for continuation and derivatives of potential fields. Jour.Korean Inst. Mining Geol., v.14, p.93-102.

Lee, H.Y., Chung, S.H. and Hyun B.K. (1985) An iterative method for the non-linear inverse problems in gravity and magnetic interpretation and its application. Jour. Korean Mining and Mineral Eng. Soc.,v.22, p.187-198(in Korean).

Lee, K.H.,Jeong, B.I.and Kim, Y.H. and Yang, S.J. (1984) A geophysical study of the Yangsan fault area. Jour.Geol.Soc.Korea, v.20, p.222-240.

Lee, K.H., Jeong. B.I.and Kim Y.H.(1985) A geophysical study of the Yangsan fault area (II). Jour.Geol.Soc.Korea,v.21,p.79-89.

Lee, K.H, Kim K.H. and Chang T.W.(1986) Seismicity of the Korean Peninsula (II) : Seismicity of the northern part of the Yangsan fault.Jour.Geol. Soc.Korea,v.22, p.347-365.

Lee, M.S. and Kang, P.J.(1964) Explanatory text of the geological map of Yangsan sheet(1: 50000). Geological Survey of Korea.

Lee, S.M.(1974) The tectonic setting of Korea with relation to plate tectonic. Jour.Geol.Soc.Korea, v.10, p.25-36.

Lee, Y.J.and Lee,I.K.(1972) Explanatory text of the geological map of Eonyang sheet(1: 50000). Geological Survey of Korea.

Lee, Y.J. and Ueda,Y.(1976) K-Ar dating on granite rocks from the Eonyang and the northwestern part of Ulsan quardrangle, Kyeongsangnam-do, Korea. J. Korean. Inst. Mining Geol.,v.9, p.127-134.

Malin, S.R.C. and Barraclough, D.R.(1981) An algorithm for synthesizing the geomagnetic field. Computers and Geosciences, v.7, p.401-405.

Min, K.D. and Kim, J.W. (1987) Gravity measurement and interpretation of the subsurface structure of the Kyongsang basin between Masan- Busan area. Jour. Korean Inst. Mining. Geol., v.20, p. 203 -209 (in Korean).

Min, K.D. and Chung, C.D.(1985) Gravity survey on the subsurface structure between Weakwan-Pohang in Kyeongsang Basin. Jour. Korean Inst. Mining. Geol.,v.18, p.321-329(in Korean).

Olorunfemi, M.O.,Olarewaju, V.O. and Avci, M. (1986) Geophysical investigation of a fault zone. Geop. Prosp.,v.34, p.1277-1284.

Otsuki, K. and Ehiro, M.(1978) Major strike-slip faults and their bearing on spreading in the Japan Sea. In : Geodynamics of the Western Pacifics. p. 537-552.

Manuscript received 21 November 1991

양산 단층에 대한 자력탐사 연구

권 병두 · 이 기원

요약 : 경상분지내에서 가장 뚜렷한 선구조로 나타나는 양산 단층이 지나는 곳으로 생각되는 네 지역을 선정하여 육상자력탐사를 실시하였다. 정성적 분석을 위한 자료처리과정으로는 표준자기장 (IGRF) 보정, 상향 연속과 자극화 변환을 수행하였고, 정량적 해석을 위해서는 수평 2층 지하 지질구조에 있어서 하부층까지의 심도를 모델변수로 하는 비선형 자동 역산법을 적용하였다. 육상자력 이상도의 상향 연속 결과와 동일 지역에서 수행된 항공 자력 탐사자료를 비교한 바에 의하면 두 자료의 유사도가 비교적 높게 나타났다. 네 곳의 탐사지역내에서 양산 단층의 주향은 북동6°-15°의 경향이 우세하게 나타났으며, 단층의 경사는 지역적인 암상의 변화에도 불구하고 수직내지 약간 동쪽 방향의 경사를 갖는 것으로 나타났다. 탐사 지역중 가장 북쪽에 위치하는 안강부근의 제 1 탐사지역에서는 단층구조에 의한 자력효과가 화성암의 관입에 의한 효과와 함께 나타난 복잡한 양상을 띠며, 언양부근의 제 2 탐사 지역에서는 단층면을 따라 약 200 - 300 미터의 폭을 갖는 화산성, 혹은 화성 기원의 관입이 일어난 것으로 보인다. 용연 부근의 제 3 지역에서는 다른 지역과는 달리 단층운동에 의한 것으로 생각되는 파쇄대가 약 600 - 700 미터 정도의 폭으로 비교적 뚜렷하게 나타났다. 가장 남쪽에 위치하는 양산부근의 제 4 지역에서는 안산암 시료가 매우 큰 대자율 값을 보이며, 본 연구 결과 이 지역의 단층선은 기존 연구에서 제시된 단층선보다 약 500 미터 정도 동쪽으로 치우쳐 나타난다.